

A Singlet Oxygen Image with 2.5 μm Resolution

Lars Klemmt Andersen, Zhan Gao, Peter R. Ogilby,* Lars Poulsen, and Ingo Zebger

Department of Chemistry, University of Aarhus, Langelandsgade 140, DK-8000 Århus, Denmark

Received: May 2, 2002

Upon irradiation of a photosensitizer, singlet molecular oxygen has been detected via its $a^1\Delta_g \rightarrow X^3\Sigma_g^-$ phosphorescence with a microscope. Using this tool, a singlet oxygen image with 2.5 μm resolution has been constructed of a phase-separated toluene/water mixture. For the $a \rightarrow X$ transition at $\sim 7850 \text{ cm}^{-1}$ ($\sim 1270 \text{ nm}$), a lateral resolution of 2.5 μm is close to the diffraction limit of $\sim 1.5\text{--}2.0 \mu\text{m}$.

Introduction

Singlet molecular oxygen ($a^1\Delta_g$) is an important intermediate in many chemical and biological processes,¹ in part, because of its unique reactivity that can result, for example, in polymer degradation² or the death of biological cells.^{3,4} Moreover, in many systems, the behavior of singlet oxygen is influenced by microscopic inhomogeneities and phase-separated domains, and reactions can be important only in specific locations.^{5,6} Thus, much would be gained if singlet oxygen could be directly monitored from such systems with spatial resolution.

We have embarked on a multifaceted program to develop optical microscopes capable of detecting singlet oxygen with spatial resolution. By extension, such microscopes could also yield concentration profiles of ground-state oxygen ($X^3\Sigma_g^-$), whose behavior likewise depends on sample inhomogeneities, particularly in biological matter.⁷ To this end, we have established that singlet oxygen can be detected with a microscope in a time-resolved absorption experiment using the $a^1\Delta_g \rightarrow b^1\Sigma_g^+$ transition at $\sim 5200 \text{ cm}^{-1}$.⁸ Unfortunately, the spatial resolution available with this tool is currently limited to a spot size of $\sim 150 \mu\text{m}$ and a volume of $\sim 20 \text{ nL}$. In a separate effort, we have established that singlet oxygen can be detected in a time-resolved experiment by its $a^1\Delta_g \rightarrow X^3\Sigma_g^-$ phosphorescence at $\sim 7850 \text{ cm}^{-1}$ upon two-photon, nonlinear excitation of a sensitizer.^{9,10} In this case, where the spatial resolution is defined by a focused laser used to irradiate the sensitizer, the prospect of creating singlet oxygen images with submicrometer lateral resolution can be considered.

For the present study, we set out to monitor singlet oxygen in a steady state $a \rightarrow X$ phosphorescence experiment. We now report that singlet oxygen can be detected upon irradiation of phase-separated toluene/water mixtures that contain a photosensitizer, and that singlet oxygen images of these heterogeneous samples can be constructed with 2.5 μm spatial resolution. For the $a \rightarrow X$ transition at $\sim 7850 \text{ cm}^{-1}$ ($\sim 1270 \text{ nm}$), a lateral resolution of 2.5 μm is close to the diffraction limit which, depending on the numerical aperture of the optics used, is $\sim 1.5\text{--}2.0 \mu\text{m}$.

Experimental Section

In this study, $\text{O}_2(a^1\Delta_g)$ was produced upon irradiation of the sensitizer 5,10,15,20-tetraphenyl-21H,23H-porphine (TPP) dissolved in toluene at a concentration of $9 \times 10^{-4} \text{ M}$. Hetero-

geneous, phase-separated samples were prepared by mixing the sensitizer/toluene solution with water in a 100 μm path length cell. TPP is not soluble in water and, thus, remains in the toluene phase.

Experiments were performed using a modified Olympus inverted microscope (model IX70). Data were obtained using objectives with infrared optics that had a magnification of either 10 \times or 20 \times and numerical apertures of 0.25 and 0.40, respectively (Olympus LMPlan IR). Transmission-based images of the sample in the visible region of the spectrum were obtained by back-lighting the sample and then using a digital camera to record the image (Nikon Coolpix 990).

Sample Stage. The sample was mounted on a movable x - y stage directly above the microscope objective. For these preliminary experiments, the sample was translated manually using micrometer screws, and the position was quantified visibly using a calibrated grid.

Sensitizer Irradiation. A 75 W steady-state Xe lamp (Osram XBO) was used to irradiate TPP. The output of this lamp was coupled onto the sample through the microscope objective using a dichroic mirror that reflected visible light (model 780dcxru, Chroma Technology Corporation). A water filter (2 cm path length), KG-2 and KG-1 filters (Schott), and a hot mirror (CVI) removed the infrared radiation. The combination of these optical elements established that the sample was exposed to light over the range 400–700 nm.

Singlet Oxygen Detection. Luminescence from the sample was collected by the microscope objective and transmitted through the same dichroic optic used to reflect the output of the Xe lamp. Spectral discrimination for the near-IR phosphorescence of $\text{O}_2(a^1\Delta_g)$ was achieved using an interference filter centered at 7875 cm^{-1} with a full-width-at-half-maximum of 310 cm^{-1} (Barr Associates), and the resultant light was coupled onto a custom-made InGaAs linear array detector (a modified OMA V from Princeton Instruments/Roper) operated at $-100 \text{ }^\circ\text{C}$. The detector array contained 512 elements (i.e., pixels), each of which was $50 \mu\text{m} \times 50 \mu\text{m}$. The spatial resolution available in this experiment is defined by the combination of the size of the elements in the detector array and the objective magnification and, for data recorded using the 20 \times objective, yields a resolution of 2.5 μm .

Data Handling and Image Construction. The software package WinView (Princeton Instruments/Roper) was used for the control and readout of the array detector. Subsequent manipulations were performed using MatLab (the MathWorks, Inc.).

* To whom correspondence should be addressed.

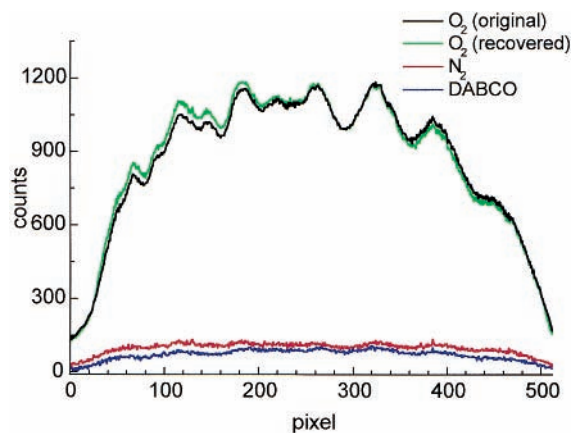


Figure 1. Plot of the light intensity detected by the InGaAs array against the individual pixels in the array. Data were recorded upon irradiation of TPP dissolved in toluene. The intensity fluctuations, including the fall off on the edges, are due to inhomogeneities in the Xe lamp and, if desired, can be normalized using a flat-field correction in the data handling software. Experiments were performed with samples exposed to oxygen and nitrogen, as well as with a sample to which the singlet oxygen quencher DABCO had been added. For the sample that had been exposed to nitrogen, the signal was recovered upon bubbling with oxygen. These particular data were recorded in a 90 s exposure time using a 1 mm path length cell, and because of the high signal level, “hot” pixels are not as apparent.

Materials. TPP (> 99%, Aldrich), DABCO (98%, Aldrich), and toluene (HPLC grade, Aldrich) were used as received. Deionized water was used from our in-house supply.

Results and Discussion

Upon irradiation of TPP dissolved in oxygenated toluene, we were able to detect a near-IR signal with the InGaAs array that can be assigned to singlet oxygen phosphorescence (Figure 1). Specifically, the signal at $\sim 7850\text{ cm}^{-1}$ disappeared upon equilibrating the sample with an atmosphere of nitrogen and, independently, upon the addition of a known singlet oxygen quencher, 1,4-diazabicyclo[2.2.2]octane (DABCO). Moreover, for the sample that had been equilibrated with nitrogen, we were able to recover the signal upon bubbling with oxygen (Figure 1).

When a heterogeneous, phase-separated sample was positioned such that the array detector cut across a water/toluene phase boundary as well as a Teflon gasket at the edge of our cell, the expected changes in signal intensity were clearly observed (Figure 2). Specifically, the singlet oxygen signal was observed from the toluene phase in which TPP was dissolved, whereas the signal was not observed from the water phase and from the domain with the Teflon gasket. In this example, where the data were recorded using the $20\times$ objective, the water/toluene boundary is resolved using ~ 10 pixels in the detector array. Thus, at $2.5\text{ }\mu\text{m}/\text{pixel}$, this phase boundary is perceived to occur over a distance of $\sim 25\text{ }\mu\text{m}$ and reflects the fact that, in the volume from which data were collected, the boundary is curved (i.e., we are looking at the edge of a “bubble”). This latter point is also evident in the visible image of the sample in Figure 2. The toluene/Teflon boundary is likewise not sharp.

When the sample is translated laterally on the microscope stage, a $\rightarrow X$ phosphorescence from successive “slices” in the sample can be recorded and combined to build a singlet oxygen image of the sample. Two such images are shown in Figures 3 and 4 along with transmission-based images of the sample that were recorded in the visible region of the spectrum. For these

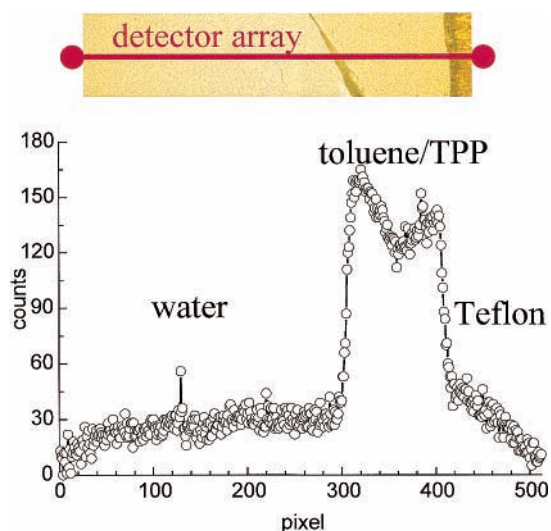


Figure 2. Plot of the light intensity detected by the InGaAs array against the individual pixels in the array. Data were recorded from a heterogeneous, phase-separated sample positioned such that the array cut across a water/toluene phase boundary and across a boundary between the toluene solution and a Teflon gasket in our sample cell (see transmission-based visible image of the sample). Data were recorded in a 90 s exposure time. “Hot” pixels in our detector array are also evident in this plot (i.e., pixels 129 and 385). As in Figure 1, a flat-field correction was not applied to the data.

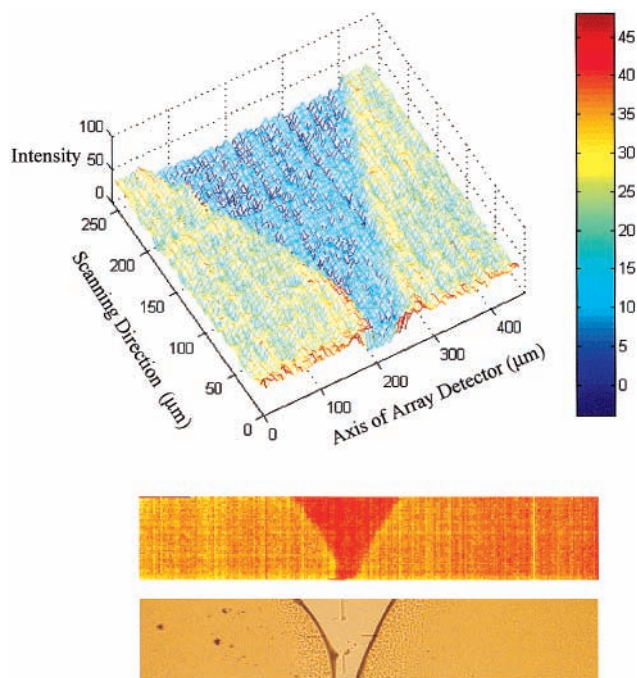


Figure 3. Images of a “v-shaped” water channel between two toluene domains. The bottom panel shows a transmission-based image of the sample recorded in the visible region of the spectrum. The middle and top panels show images of this same sample constructed using the $\sim 7850\text{ cm}^{-1}$ phosphorescence of singlet oxygen detected by the InGaAs array (only a portion of the data recorded by the array is shown). The singlet oxygen signal originates from the toluene domains, whereas the “v-shaped” domain in the center is void of singlet oxygen. The colors chosen for the singlet oxygen images are arbitrary and reflect the intensity scale used.

singlet oxygen images, data from each slice in the sample was recorded using an exposure time of 30 s.

In Figure 3, data were recorded using the $10\times$ objective and have a resolution of $5\text{ }\mu\text{m}/\text{pixel}$ and $5\text{ }\mu\text{m}/\text{slice}$. In this sample, one sees a water channel between two toluene domains. Thus,

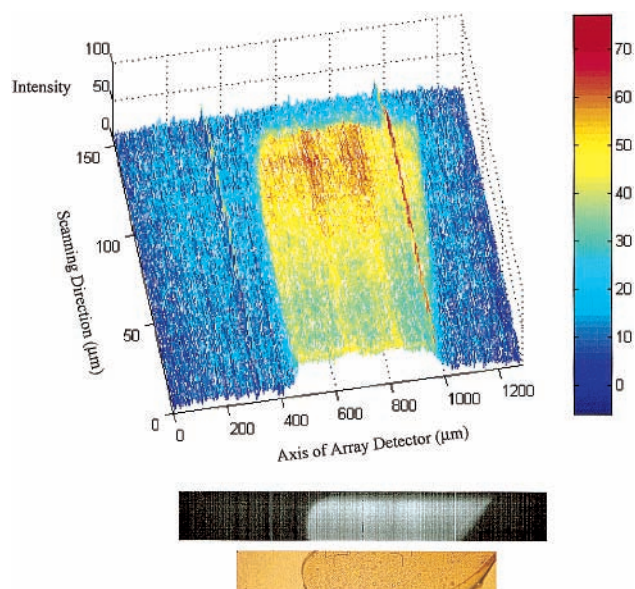


Figure 4. Images of a toluene domain surrounded by water. The bottom panel shows a transmission-based image of the sample recorded in the visible region of the spectrum. The middle and top panels show images of this same sample constructed using the $\sim 7850\text{ cm}^{-1}$ phosphorescence of singlet oxygen detected by the InGaAs array. The singlet oxygen signal originates from the toluene domain, whereas the surrounding water domain is void of singlet oxygen. The colors chosen for the singlet oxygen images are arbitrary, and reflect the intensity scale used. The effects of “hot” pixels in our InGaAs array are seen as ridges and lines in the singlet oxygen images (i.e., ridges seen at the 322.5 and 962.5 μm marks). As in Figure 1, a flat-field correction was not applied to the data.

there is no singlet oxygen in the central “v-shaped” domain. In Figure 4, data were recorded using the $20\times$ objective and have a resolution of $2.5\ \mu\text{m}/\text{pixel}$ and $2.5\ \mu\text{m}/\text{slice}$. In this case, we have a toluene domain that contains singlet oxygen surrounded by water.

Two important points are illustrated by the data in Figure 4. First, two sections of our InGaAs array have “hot” pixels, in which an offset is effectively added to any information recorded. As a consequence, these pixels give rise to data with artificially

high intensity levels that appear as ridges or lines in the singlet oxygen images. Second, in the way data are presently recorded, the entire portion of the sample being imaged is irradiated by the output of the Xe lamp as the information from successive slices is collected to build up the image. Thus, irradiation-induced changes in the sample (e.g., sensitizer photochemistry) can be manifested in the singlet oxygen signal, and data recorded at early times may not properly correspond to data recorded at later times. This phenomenon is seen in Figure 4 as a change in the intensity of the singlet oxygen signal as one progresses from the bottom of the image (early times) to the top (later times).

Conclusions

We have demonstrated that $\text{O}_2(a^1\Delta_g)$ -based images of heterogeneous samples can be generated with a spatial resolution that is significant for many chemical and biological processes.

Acknowledgment. This work was supported by grants from the Danish Natural Science Research Council and from the Materials Research Program of the Technical Research Council. The authors thank Jan Thøgersen for assistance during the early stages of this work and Kirk S. Schanze for insight during the development of our microscope.

References and Notes

- (1) *Singlet Oxygen*; Frimer, A. A., Ed.; CRC Press: Boca Raton, FL, 1985; Vols. I–IV.
- (2) Scurlock, R. D.; Wang, B.; Ogilby, P. R.; Sheats, J. R.; Clough, R. L. *J. Am. Chem. Soc.* **1995**, *117*, 10194–10202.
- (3) Kochevar, I. E.; Lynch, M. C.; Zhuang, S.; Lambert, C. R. *Photochem. Photobiol.* **2000**, *72*, 548–553.
- (4) Weishaupt, K. R.; Gomer, C. J.; Dougherty, T. J. *Cancer Res.* **1976**, *36*, 2326–2329.
- (5) Lee, P. C.; Rodgers, M. A. J. *J. Phys. Chem.* **1984**, *88*, 4385–4389.
- (6) Oleinick, N. L.; Morris, R. L.; Belichenko, I. *Photochem. Photobiol. Sci.* **2002**, *1*, 1–21.
- (7) Fuchs, J.; Thiele, J. *Free Rad. Biol. Med.* **1998**, *24*, 835–847.
- (8) Andersen, L. K.; Ogilby, P. R. *Photochem. Photobiol.* **2001**, *73*, 489–492.
- (9) Frederiksen, P. K.; Jørgensen, M.; Ogilby, P. R. *J. Am. Chem. Soc.* **2001**, *123*, 1215–1221.
- (10) Poulsen, T. D.; Frederiksen, P. K.; Jørgensen, M.; Mikkelsen, K. V.; Ogilby, P. R. *J. Phys. Chem. A* **2001**, *105*, 11488–11495.